Multibody Syst Dyn (2010) 24: 347–366
DOI 10.1007/s11044-010-9217-8

# A study on wear evaluation of railway wheels based on multibody dynamics and wear computation

**João Pombo · Jorge Ambrósio · Manuel Pereira · Roger Lewis · Rob Dwyer-Joyce · Caterina Ariaudo · Naim Kuka**

Received: 19 December 2009 / Accepted: 8 July 2010 / Published online: 13 August 2010


**Abstract** The wear evolution of railway wheels is a very important issue in railway engineering. In the past, the reprofiling intervals of railway vehicle steel wheels have been scheduled according to designers' experience. Today, more reliable and accurate tools in predicting wheel wear evolution and wheelset lifetime can be used in order to achieve economical and safety benefits. In this work, a computational tool that is able to predict the evolution of the wheel profiles for a given railway system, as a function of the distance run, is presented. The strategy adopted consists of using a commercial multibody software to study the railway dynamic problem and a purpose-built code for managing its pre- and post-processing data in order to compute the wear. The tool is applied here to realistic operation scenarios in order to assess the effect of some service conditions on the wheel wear progression.

**Keywords** Railway dynamics · Multibody systems · Wheel profile wear · Traction/braking forces

## 1 Introduction

The increase of the railway transport competitiveness requires the development of sophisticated railway systems that answer to the increasing demands of modern societies. For short and medium distances, high speed trains are able to compete with the air transportation,

J. Pombo (✉) · J. Ambrósio · M. Pereira
IDMEC—Instituto Superior Técnico, Av. Rovisco Pais 1, 1049-001 Lisbon, Portugal
e-mail: jpombo@dem.ist.utl.pt
Fax: +351-218-417915

R. Lewis · R. Dwyer-Joyce
Department of Mechanical Engineering, University of Sheffield, Mappin Street, Sheffield, S1 3JD, UK

C. Ariaudo · N. Kuka
Running Dynamics—ALSTOM Ferroviaria S.p.A., Via O. Moreno 23, 12038, Savigliano (CN) Italy

having several advantages such as better energy efficiency and less impact on the environment (e.g. $CO_2$ footprint). The increase of the railway share of persons and freight transport also relies on a more efficient transport system. In order to improve its competitiveness, railway industrial integrators and research centres are investing large resources in research and development activities. These studies contribute decisively to the development of new design concepts by using advanced simulation techniques, modern production methods and innovative optimization procedures.

One of the most sensible issues in the railway industry is the impact on infrastructure of train operations and the damage on vehicles provoked by the track conditions. These issues have a significant impact on the life cycle costs of the railway networks. The consequence is that the prices billed by the infrastructure managers to the railway operators are being defined according to the damage that the trainsets are supposed to cause to the track. Therefore, the study of vehicle-track interaction is important in reducing the operation and maintenance costs, by increasing the life cycle of both vehicles and tracks, and increasing the speed, safety, and comfort indexes of the railway systems. In this regard, these studies have a significant role to play in promoting the competitiveness of the railway transportation.

During trainset operation, the wheels of railway vehicles are subjected to wear. When the worn state of the profiles reaches a limit value defined by international standards [1], the wheels have to be reprofiled. In the railway community, it is well known that there are mission profiles (operation conditions, track geometry, wheel-rail profiles, etc.) where some trainsets require the reprofiling of their wheelsets after only 80.000 km of service, whereas others are able to operate in similar conditions for more than 400.000 km without need such maintenance procedure. Furthermore, the railway wheels can only be reprofiled 3 or 4 times and the wheelset substitution is very expensive. The excessive wheel wear implies that, conversely, also the rails are subjected to premature deterioration. Thus, the complete characterization of the wheel wear problem allows tackling the rail wear problem as well. It is, therefore, essential to acquire a better understanding on how the wheel wear evolution is affected by the mission profile of the trainsets and what is the impact of the wear growth on the dynamic behavior of railway vehicles. Such evaluation is an important contribution to optimize the rolling stock design and to enhance the construction features of the railway infrastructure.

Up to now there are no commercial computational tools able to study, according to the trainset operation conditions, the wear evolution on railway wheels and to predict the intervals between the reprofiling procedures. The work presented here resulted from a Transfer of Knowledge (ToK) project between Industry and Academia, which aimed to contribute to the development of such a tool. The objective is to improve the modelling capabilities of the tools used to study the dynamic response of railway systems in order to enhance the wheel wear prediction techniques. This ToK project was called AWARE (ReliAble Prediction of the WeAr of Railway WhEels) and it was funded by the EU to meet its transport policy objectives for improvement of efficiency and competitiveness of the European railway transportation networks.

The capability of the computational tool for wheel wear prediction, developed in the scope of project AWARE, is demonstrated here in several realistic scenarios of operation. The purpose is to evaluate the influence on the wheel wear growth of some physical parameters related to the vehicle characteristics and to the trainset service conditions. Special emphasis is given to study how the wear progression is affected by the primary suspension stiffness, rail cant, traction/braking forces, and vehicle velocity. The assessment of the wear sensitivity to each one of these railway dynamic parameters is made in terms of predicted reprofiling intervals.

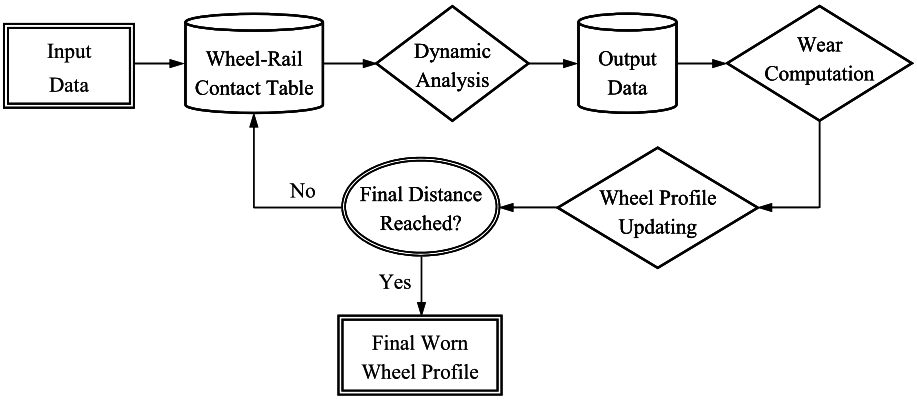


**Fig. 1** Schematic representation of the wear prediction tool

## 2 Overview of the computational tool

The computational tool developed here consists of using the commercial multibody software VAMPIRE [2–4], which is used to study the dynamics of the railway vehicles, integrated with a purpose-built wear computation module that is used to predict the wear of the railway steel wheels [5–10]. According to this strategy, an initial wheel profile is provided and the Multibody Software (MBS) runs a simulation for a pre-defined travel distance. Then the wear prediction module collects the necessary data from the dynamic analysis results and calculates the wear, i.e., the amount of material to be removed from the wheel surfaces. The resulting updated profiles are then used as input for a new dynamic analysis in the MBS. This methodology, represented in Fig. 1, is repeated as many times as necessary until reaching the distance required for the wear study.

In real situations, trainsets are operated on different tracks. Therefore, when predicting the wear evolution on the wheels of a railway vehicle, this issue has to be considered and the wear studies should be performed using track models (geometry and characteristics) that represent the real operation conditions. In the computational tool presented here, there are no limitations with respect to the length of the track models or to the number of models to use. In fact, after each simulation with the MBS, the wheel profiles are updated and used as input for a new dynamic analysis in the MBS. This new dynamic analysis can be performed with the same track model or with a different one. This approach allows computation of the wheel wear with more precision by reproducing the real conditions that the railway vehicles experience during their operation. The result is thus the wheel profile evolution, in respect of distance run, for the vehicle mission specified by the user.

A schematic representation of the wear computational tool is presented in Fig. 1 and it consists of the following steps [7–10]: (1) Prepare the input data for the computation; (2) Obtain the wheel-rail contact table; (3) Run the multibody dynamic analysis; (4) Read the dynamic analysis output data; (5) Compute the quantity of worn material; (6) Update the wheel profiles. The wear prediction study ends when the total simulated distance matches the total distance defined by the user.

The wear computation block, represented in Fig. 1, is the core of the wear prediction tool as it computes the amount of worn material to be removed from the wheel surfaces, starting from the MBS dynamic results. It is divided into 3 parts: (i) Contact model; (ii) Wear function; (iii) Wear distribution. The contact model processes the dynamic analysis results

**Table 1** Equations governing the wear function

| Wear regime | Wear range $T\gamma/A$ (N/mm$^2$) | Wear rate (μg/m/mm$^2$) |
|---|---|---|
| Mild | $\frac{T\gamma}{A} < 10.4$ | $5.3\frac{T\gamma}{A}$ |
| Severe | $10.4 \leq \frac{T\gamma}{A} < 77.2$ | 55.0 |
| Catastrophic | $\frac{T\gamma}{A} \geq 77.2$ | $61.9\frac{T\gamma}{A}$ |

to obtain the wheel-rail contact parameters [11–15]. The wear function uses these contact parameters as input to compute the quantity of worn wheel material [5, 6, 8–10]. The wear distribution allocates the quantity of worn material along the wheel profile.

The wear functions relate the energy dissipated in the wheel-rail contact patch with the amount of worn material to be removed. In general, these wear laws use the normal and tangential forces and the relative slip velocities (creepages), as input to compute the wear. In the literature [5, 8–10, 16–26], different methods for estimating wear of railway wheels can be found. These methods are based on real wear data acquired using different experimental techniques.

In this work, the wear function developed by the University of Sheffield [5, 10] is used. It relates the wear rate, representing the weight of lost material (μg) per distance rolled (m) per contact area $A$ (mm$^2$), to the product $T\gamma$, where $T$ is the tangential contact force and $\gamma$ is the global creepage. This formulation is based on twin disk experimental data acquired from the contact between discs made of R8T wheel material and UIC60 900A rail material. These experimental tests have identified three wear regimes, mild, severe, and catastrophic, for the contact between wheel and rail materials. Notice that these materials are the ones used to assemble the vehicles and tracks considered here. The equations governing the University of Sheffield wear function are defined in Table 1.

## 3 Wear parameters for steel railway wheels

During service, the steel wheels of railway vehicles are subjected to wear. These changes in the profile geometry affect the dynamic behavior of the whole trainset and, consequently, their evolution has to be assessed. A common method for wheel wear geometric analysis is provided in the UIC 510-2 leaflet [1]. According to this standard, a good and pragmatic approach for the geometric characterization of the wheels wear is based on the measurement of the profile parameters $Sh$, $Sd$, and $qR$. These parameters are represented in Fig. 2, where $Sh$ is the flange height, $Sd$ represents the flange thickness, $qR$ is the flange slope quota, $D$ is the wheel diameter, $\Delta D$ represents the deviation of roundness and $d$ is the wheelset external gauge. The quantities $L_1$, $L_2$, and $L_3$ are the reference quotas for the measurement of the wheel wear parameters.

The wheel wear characterization based on programmed measurements of the geometrical parameters $Sh$, $Sd$, and $qR$ is widely used by the railway industry. Such assessment is a relevant criterion to evaluate the wear state of the wheels. This approach consists of monitoring periodically the geometrical parameters of the wheel profiles in order to check if they have reached the safety limit values defined by the technical specifications. When that happens, it means that the wheels have to be reprofiled. According to the UIC 510-2 [1], the admissible values for parameters $Sh$, $Sd$, and $qR$ are defined in Table 2.

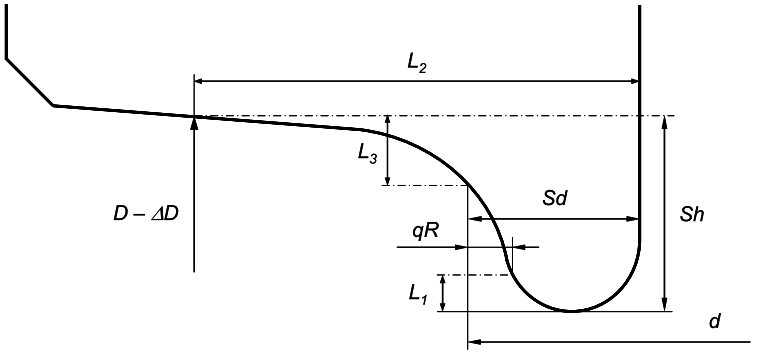


**Fig. 2** Wear parameters for railway steel wheels

**Table 2** Admissible values for wheel wear parameters

| Wheel profile S1002 | Wear parameters (mm) | | | Reference quota (mm) | | | Flange angle |
|---|---|---|---|---|---|---|---|
| | *Sh* | *Sd* | *qR* | $L_1$ | $L_2$ | $L_3$ | |
| New profile (mm) | 28 | 32.5 | 10.8 | | | | 70° |
| $(760 < D < 1000)$ | | | | 2 | 70 | 10 | |
| Allowable (mm) $(840 < D < 1000)$ | $\leq 36$ | $\geq 22$ | $> 6.5$ | | | | – |

The measurement of the wear parameters *Sd* and *qR* allows predicting the influence of the wear state of the wheel profiles on the dynamic behavior of the railway vehicles. For example, the flange thickness *Sd* is very important as it limits the lateral clearance of wheelset with respect to the track, which influences the vehicle stability. The flange slope quota *qR* is also an important parameter. If it is too small, the wheel flange will be almost vertical, which implies that the transitions (switches crossing) and the flange contacts will occur abruptly. Such a situation originates very high contact forces that damage both vehicle and infrastructure. From Table 2, it is also noticeable that the difference between the new and the allowable values for the flange height *Sh* reveals that the maximum wear depth admissible in the wheel tread is 8 mm.

## 4 Wheel wear studies

During project AWARE, the computational tool described here allowed performing numerous wear evolution studies of two railway vehicles that are representative of different trainset layouts used by the railway industry. The purpose is to evaluate how the wheels wear is influenced by several parameters associated to the vehicles, track characteristics, and service conditions. In the following, some selected results of these studies are presented.

### 4.1 Influence of primary suspension stiffness

The trainset considered to study the influence on wear growth of the primary suspension stiffness is a three-vehicle articulated trainset with Jacobs's bogies represented in Fig. 3. It is

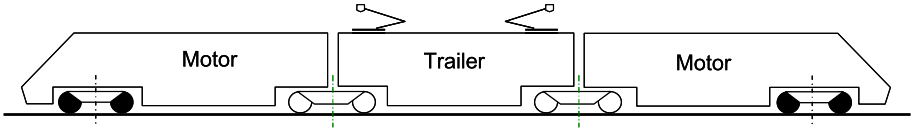


**Fig. 3** Vehicle 1—Articulated trainset with Jacob's bogies

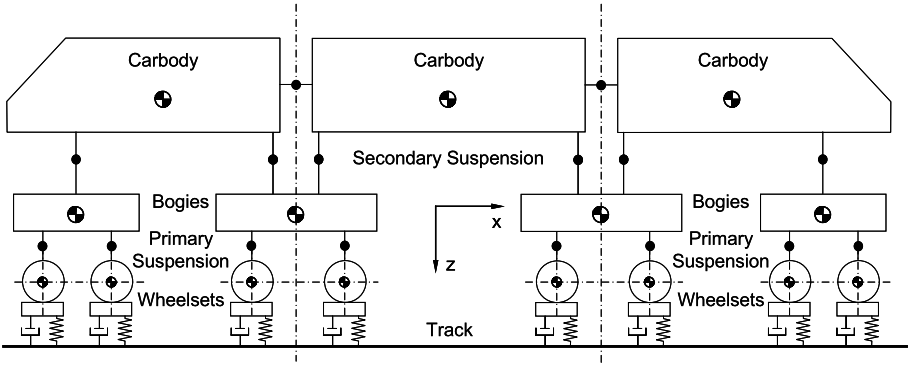


**Fig. 4** Multibody model of Vehicle 1

composed of four bogies, with the two bogies of the extremities being motorized (wheelsets are represented in black), and the two middle bogies being trailers (with wheelsets represented in white). Due to its configuration, the dynamic behavior of each vehicle of the trainset affects the performance of the others. Therefore, the whole trainset has to be considered when building the vehicle model, which is used by the MBS to run the dynamic analyses during the wear studies. Hereafter it is named as Vehicle 1.

The 3D model of Vehicle 1 is built using a multibody approach [27–32], as depicted in Fig. 4. This methodology allows accurate representation of the mass and inertia properties of the structural elements that compose the vehicle. It also includes the kinematic joints, which control the relative motion between the bodies, and the force elements, that represent suspension components of vehicle.

Vehicle 1 has two levels of suspension, the primary and the secondary. The primary suspension elements connect the bogie frame to the axleboxes of the wheelsets and are the main responsible for the steering capabilities and stability behavior of the whole trainset. The carbody is supported by the bogies through secondary suspension elements. Their main function is to minimize the vibrations induced by the track on the passengers' compartment, improving the comfort and reducing the problems associated with structural fatigue.

The multibody model of the railway vehicle represented in Fig. 4 is composed by 15 rigid bodies. These are used to represent 3 carbodies, 4 bogie frames and 8 wheelsets. The rigid bodies are connected by elastic and viscous components, having linear and nonlinear characteristics.

One of the main issues in railway dynamics is the compromise between running on straight tracks and negotiating curves. In a straight track, it is advantageous to have a rigid primary suspension as it improves the vehicle stability. In a bogie with these characteristics, the yaw motions of the wheelsets relative to the bogie frame are very restricted. Such bo-

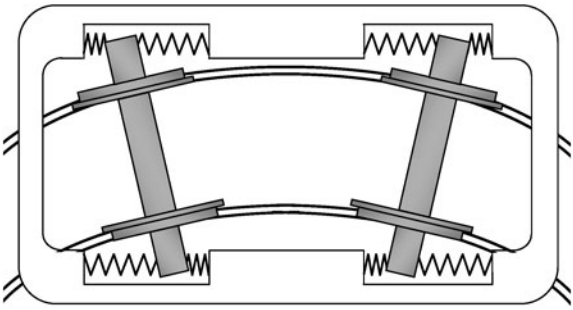

**Fig. 5** Yaw motion of wheelsets when negotiating a curve

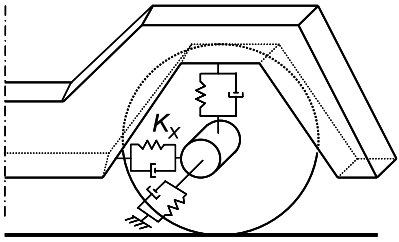


**Fig. 6** Representation of the primary suspension elements

gies have good ride stability properties and originate a rather high critical speed, but their performance in curves is poor [33, 34].

In a curve, it is useful to have a flexible primary suspension in order to improve the curve negotiation performance of the trainset. This design principle allows a significant yaw motion of the wheelsets relative to the bogie frame and a good curving performance is achieved, as represented in Fig. 5. However, instability may occur on tangent track if the longitudinal stiffness is too low [33, 34].

The influence of the primary suspension stiffness on wheel wear progression is studied here by considering Vehicle 1 assembled with two different values for the longitudinal stiffness $Kx$. The primary suspension parameter $Kx$, represented in Fig. 6, is changed in both motor and trailer bogies as follows:

- Reference value: $Kx = K$
- Modified value: $Kx = K/2$

The comparative wear study is made on the track between the cities of Cuneo and Ventimiglia, from the Italian railway network. This track has about 96 km length and it is particularly curved, with 61% of its curves having radii with less than 450 m, as represented in Fig. 7. The vehicle is initially equipped with new wheels, with S1002 profile [1], and the track model is assembled with UIC60 rails [35] with 1/20 cant.

The wear computation is carried out by performing several outward and return journeys on the Cuneo–Ventimiglia track until reaching the total distance of 5000 km. The velocity of Vehicle 1 is varied between 80 and 95 km/h along the track length, which is in conformity with the service conditions on this track.

In Fig. 8, the wear results for the first wheelset of Vehicle 1, assembled with different stiffness values for the primary suspension, are presented. On the top of the figure, the comparison between the wear depth values is shown. These results are presented as a percentage of the maximum wear depth value obtained. The new and the worn profiles, on the left and right wheels, are given on the bottom of Fig. 8. The results show that the levels of wear on

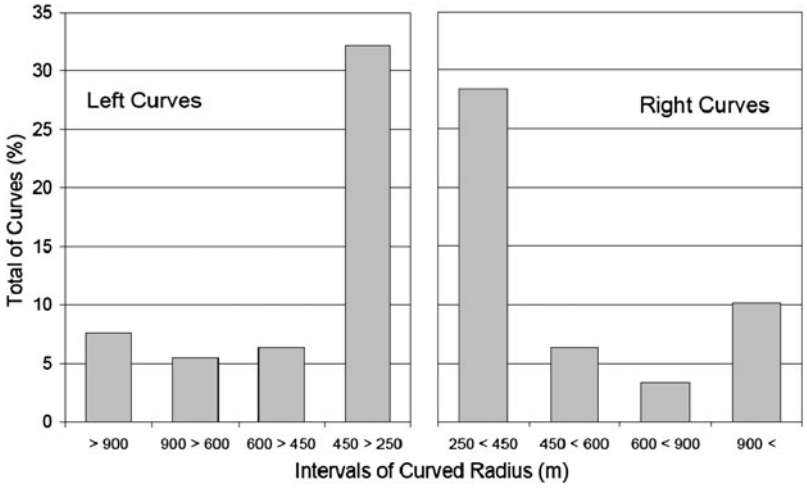


**Fig. 7** Curve radii distribution of the track

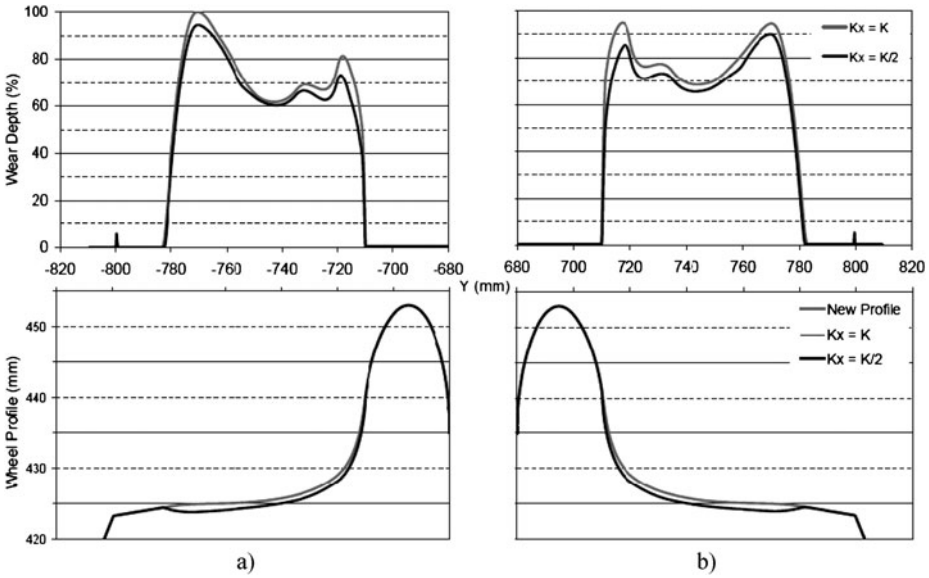


**Fig. 8** Wear results with different stiffness values of primary suspension on: (**a**) *Left wheel*; (**b**) *Right wheel*

both tread and flange zones are higher with the stiffer primary suspension. It is also observed that the wear distribution along the profiles is similar in the two cases.

In order to assess how the primary suspension stiffness affects the reprofiling intervals of the wheelsets of Vehicle 1, the worn profiles of all wheels are analyzed. This evaluation is made by studying the evolution of the wheel wear parameters $Sh$, $Sd$, and $qR$ and by comparing them with the admissible values defined in Table 2. Such an approach can be used to predict when the profile parameters reach the limit values, and consequently to estimate the corresponding reprofiling intervals. The results obtained with this methodology

**Table 3** Summary of the influence of primary suspension stiffness on wear

| Primary suspension | Longitudinal stiffness | Reprofiling interval variation |
|---|---|---|
| Reference suspension | $K$ | +16.5% |
| Modified suspension | $K/2$ | |

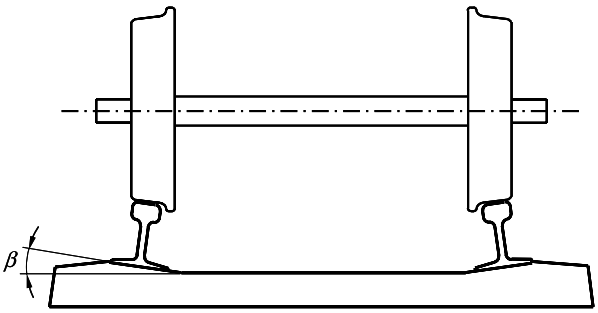


**Fig. 9** Rails mounted with an inclination inwards

are summarized in Table 3. It is observed that the vehicle assembled with the softer primary suspension has an interval between reprofiling maintenance procedures that is 16.5% larger than the one of the vehicle equipped with the stiffer suspension.

### 4.2 Influence of rail cant

In modern railway networks, the rail profiles are shaped to fit together with the geometry of the wheels, especially when they are worn. In most cases, rails are mounted with an inclination inwards, as shown in Fig. 9, because the wheel profiles are coned. Usually the rail cant varies between 1/40 and 1/20, but in some turnouts, rails may be mounted without inclination. In the Italian railway network, a 1/20 rail cant is usually used, whereas the German tracks are in general assembled with a rail cant of 1/40.

The purpose now is to evaluate the wheel wear sensitivity to the rail inclination. For this purpose, two wear computations are performed considering exactly the same service conditions, except the rail cant that has the following values:

- Reference rail cant 1/20: $\beta = 0.050$ rad $= 2.86°$;
- Alternative rail cant 1/40: $\beta = 0.025$ rad $= 1.43°$.

In Fig. 10, the UIC 60 rails mounted with an inclination inwards of 1/20 and 1/40 are represented. Despite the rail profiles being the same, the different cant influences the wheel-rail contact geometry, and consequently the equivalent conicity [33, 36, 37], which is an important parameter used to evaluate the running stability of railway vehicles. The importance of the equivalent conicity results from the fact that the steering mechanism of a wheelset depends on the difference in rolling radii between left and right wheels.

In general, the equivalent conicity is a nonlinear function of the wheelset lateral displacement and it depends on the geometric combination of both wheel and rail profiles. It also depends on the wheelset inside gauge, flange thickness, rail cant, and track gauge. In Fig. 11, the evolution of the equivalent conicity for a wheelset assembled with S1002 wheels and for UIC 60 rails with cant of 1/20 and of 1/40 is presented. It is observed that, for example, for 3 mm wheelset lateral shift with respect to the track centerline, the equivalent conicity

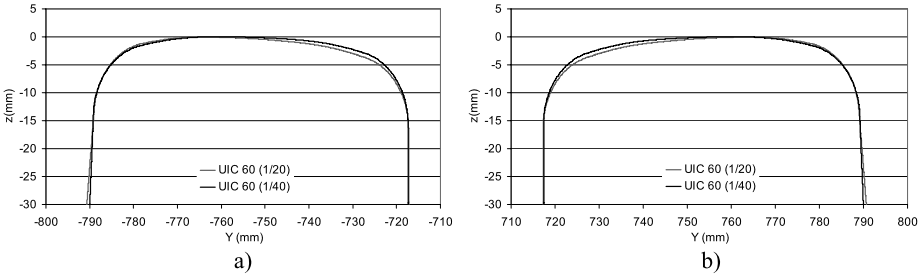


**Fig. 10** UIC 60 rails mounted with an inclination of 1/20 and 1/40: (**a**) *left*; (**b**) *right*

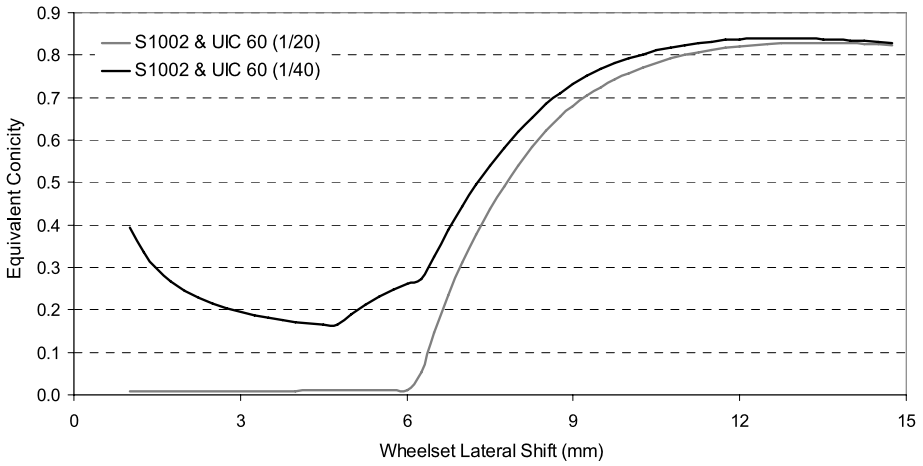


**Fig. 11** Equivalent conicity for wheel profile S1002 and rails UIC 60 with cant of 1/20 and 1/40

for 1/20 rail cant is 0.01 whereas, for 1/40 rail cant, it has a value of 0.2. As the rail cant originates differences in the equivalent conicity, it will also affect the dynamic behavior of the railway vehicles. This fact has repercussions on the wear evolution of the wheels.

The trainset considered here to study the consequences of the rail cant on the wheel wear growth is a non-articulated conventional trainset composed of seven vehicles interconnected by linking elements, as represented in Fig. 12.

Due to the trainset configuration, it is assumed that, concerning the wear studies performed here, the dynamic behavior of each vehicle has a non-significant influence on the others. According to this assumption, each vehicle of the trainset can be studied independently, as shown in Fig. 13. In this way, the vehicle model considered is composed only by one unit of the trainset, called hereafter as Vehicle 2. This composition is a motor vehicle that is assembled with two trailer wheelsets, represented in white, and two motor wheelsets, represented in black.

The 3D model of Vehicle 2 is built using a multibody approach, as depicted in Fig. 14. The vehicle model is composed by 1 carbody, 2 bogie frames, 2 carbody bolsters, 4 traction rods, and 4 wheelsets. It also includes the kinematic joints, which control the relative motion between the bodies, and the force elements, that represent suspension components of vehicle.

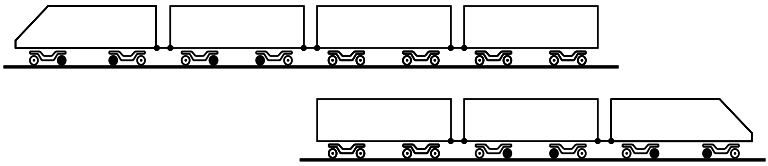

**Fig. 12** Non-articulated conventional trainset

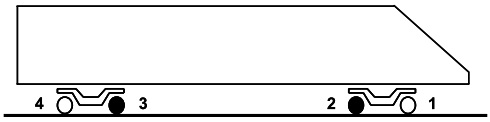


**Fig. 13** Vehicle 2—Motor vehicle of non-articulated conventional trainset

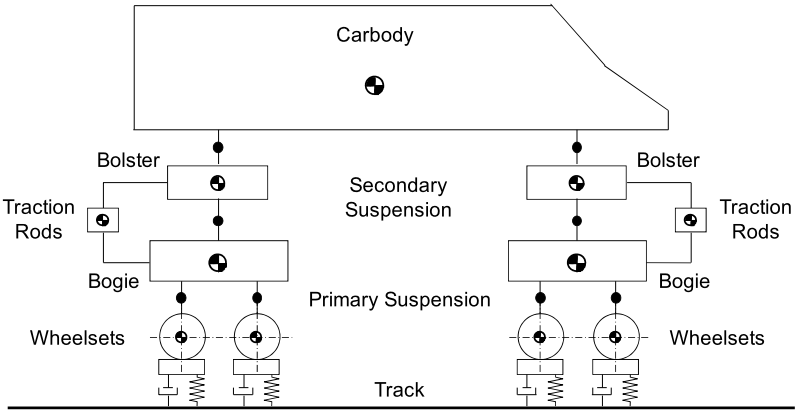


**Fig. 14** Multibody model of Vehicle 2

The primary suspension of Vehicle 2, represented in Fig. 15, is composed of two vertical coil springs, assembled laterally at each side of the axleboxes, and one vertical damper. It also includes an axle guide link system to transmit the longitudinal forces between the wheelsets and the bogie frame. The vertical displacements of the primary suspension elements are limited by a bumpstop and a liftstop, mounted at each axlebox.

The carbody is sprung against each bogie frame via a bolster and four flexi-coils. At both sides of the bogies, and assembled in parallel with each pair of coil springs, there is a vertical hydraulic damper. These elements are used for stabilization and also work as the vertical bumpstop and liftstop device of the secondary suspension. In order to guarantee a small roll coefficient, the bolsters are controlled in their roll movement by one anti-roll bar. The yaw movement of the bogies is limited through two anti-yaw dampers assembled between the carbody and each side of the bogie frames.

In Vehicle 2, the connection between the carbody and each one of the bogies is realized by a pivot shaft. This element is rigidly fixed to the carbody and is assembled vertically, passing through the bolster and bogie frame without contacting them directly, as depicted in Fig. 16. A center plate is rigidly fixed to the extremity of the pivot and it is hinged to the bogie frame by two longitudinal traction rods. This subsystem only ensures the vehicle steering functions, transmitting the in-plane loads between the carbody and bogie, but not

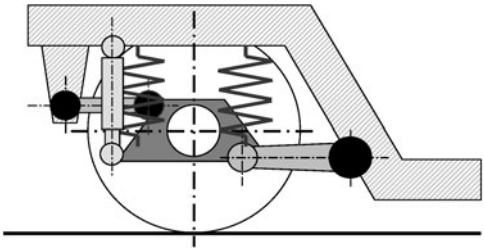

**Fig. 15** Primary suspension model of Vehicle 2

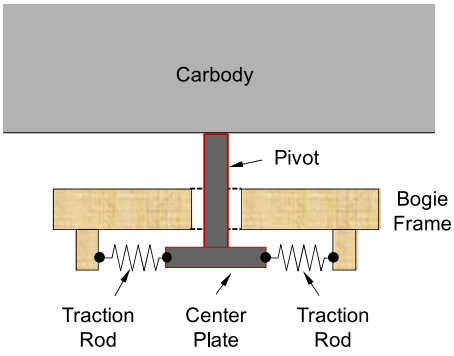


**Fig. 16** Bogie-carbody connection of Vehicle 2

the vertical loads, which are transmitted through the secondary suspension elements. The low attachment position between carbody and bogies minimizes the wheel load changes that develop during the vehicle traction and braking. The traction rods are assembled with rubber bushings at their extremities in order to ensure a better performance when the vehicle travels in small radius curved tracks. The lateral stabilization of the carbody is achieved through two pairs of transversal hydraulic dampers, assembled between the bogie frames and the carbody. The relative lateral displacement between the carbody and each bogie is limited by two transversal rubber bumpstops.

The track considered here is the one between the Italian cities of Cuneo and Ventimiglia that was described previously and which characteristics are shown in Fig. 7. The comparative wear study is carried out by performing several outward and return journeys on the track until reaching the total distance of 5000 km. In agreement with the service conditions on this track, the velocity of Vehicle 2 is varied between 80 and 95 km/h.

In Fig. 17, the wear results for the first wheelset of Vehicle 2 are presented. On the top, the comparison between the wear depth values is shown, being the results presented as a percentage of the maximum wear depth value obtained. On the bottom of the figure, the new and the worn profiles are given. The results show that a rail cant of 1/20 produces more wear on the tread zone of the wheel profiles. On the other hand, a rail inclination of 1/40 originates more wear on the flange zone.

The results from Fig. 17 can be explained by the fact that the wheels with a S1002 profile have the main part of the tread with a 1/40 cone. In such conditions, the rail with a 1/40 cant has its vertical axis perpendicular to the wheel tread, which implies that the contact area will be bigger than when using a rail with an inclination of 1/20. In order to study this issue in more detail, the variation of the contact patch on the left wheel of Vehicle 2 is shown in Fig. 18. It is observed that for a positive lateral displacement of the wheelset with respect to the track, corresponding to a tread contact, the contact patch area is bigger with a 1/40 rail cant than with a 1/20. As the contact area is larger when using a 1/40 rail inclination, the

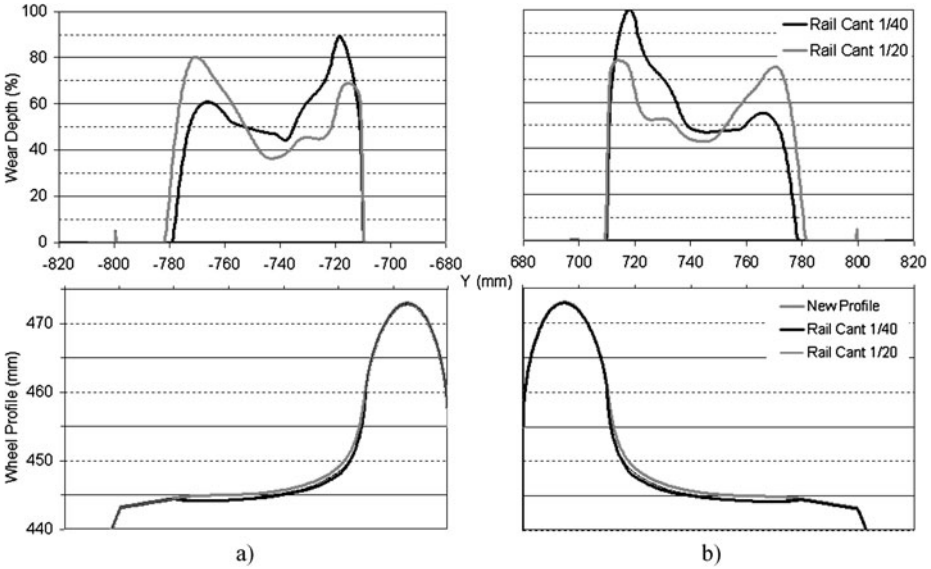


**Fig. 17** Wear results with rail cant of 1/20 and of 1/40 on: (**a**) *Left wheel*; (**b**) *Right wheel*

stresses developed in the contact patch are smaller and, consequently, less wear will arise on the wheel tread.

It should be noted here that Fig. 18 is obtained for a static computation of the wheelset. The different rail cant also influences the wheel-rail contact geometry on the flange zone of the wheel profile. In fact, the results from Fig. 18 show that for a wheelset lateral shift lower than −4.5 mm, where the flange contact is more prone to occur, the contact area is smaller when using a UIC 60 rail with 1/40 cant. This implies that higher stresses and, consequently, more wear will appear on the wheel flange when using a rail inclination of 1/40.

With the purpose of assessing how the rail cant affects the reprofiling intervals of Vehicle 2, the worn profiles of all wheels are analyzed. This evaluation is made as explained previously, i.e., by studying the evolution of the wheel wear parameters $Sh$, $Sd$ and $qR$ and by comparing them with the admissible values defined in Table 2. The results obtained in this way are summarized in Table 4, where the values of the equivalent conicity correspond to a wheelset lateral shift of 3 mm. It is observed that the use of a rail cant of 1/40 instead of 1/20 increases by 10.6% the reprofiling interval of the wheelsets of Vehicle 2.

### 4.3 Influence of traction/braking forces

The aim of this case study is to evaluate the wheel wear sensitivity to the traction and braking forces that are applied on the wheelsets of the railway vehicles during their operation. For this purpose, two wear computations are performed. In one case, no traction/braking forces are considered whereas, in the other case, these loads are applied to the vehicle wheelsets during the dynamic analysis. All other service conditions and analysis parameters required for the wear studies remain unchanged.

The wear evolution studies are executed by performing several outward and return journeys on the Cuneo–Ventimiglia track, which is characterized in Fig. 7, until reaching the total distance of 5000 km. The vehicle model considered here is Vehicle 2. The velocity

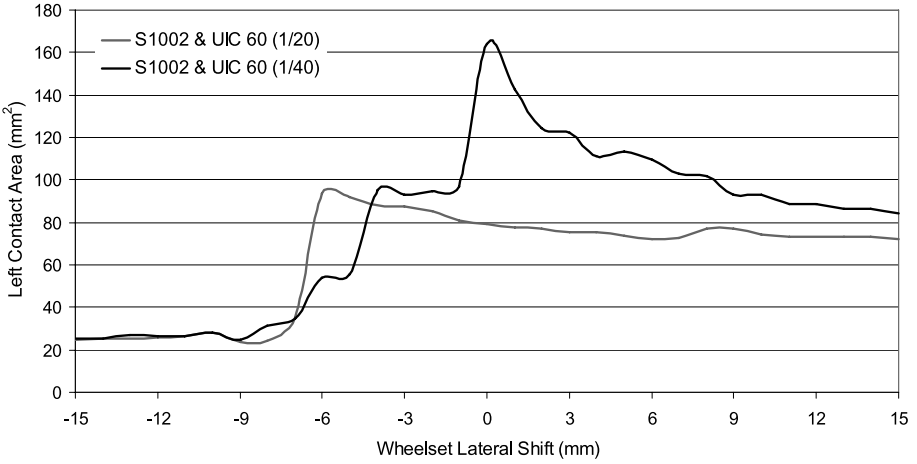


**Fig. 18** Contact area on the left wheel of Vehicle 2

**Table 4** Summary of the influence of rail cant on wear

| Rail cant | Equivalent conicity | Reprofiling interval variation |
|---|---|---|
| Reference cant (1/20) | 0.01 | +10.6% |
| Alternative cant (1/40) | 0.20 | |

profile along the track length and the traction and braking forces that are applied during the wear computation are presented in Fig. 19. This information is collected by the railway operator and it includes the braking and accelerations resultant from the train stops in the railway stations that exist in the Cuneo–Ventimiglia track. It should be noted that the effects of wheel locking, during braking, or wheel sliding, during traction, are not considered in this study.

The traction and braking forces are accounted for by applying the following torques on wheelsets of Vehicle 2, which is represented in Fig. 13:

- Traction Forces: Applied on the motor wheelsets;
- Electrical Braking Forces: Applied on the motor wheelsets;
- Mechanical Braking Forces: Applied on motor and trailer wheelsets since both are equipped with brake discs.

In the comparative wear study performed here, only the motor wheelsets (2 and 3 in Fig. 13) are studied due to the fact that they are applied with traction forces, electrical braking forces and mechanical braking forces, whereas the trailer wheelsets (1 and 4) are only subjected to the mechanical brakes. In addition, Fig. 19d) reveals that this braking system is only used four times during trainset operation and for very short periods. Therefore, the traction/braking forces will have negligible consequences on the wear growth of the trailer wheelsets when compared with the repercussions on the motor ones. In Fig. 20, the wear depth results and the new and worn wheel profiles are presented for the second wheelset of Vehicle 2. The results show that the levels of wear are slightly higher when considering the traction/braking forces.

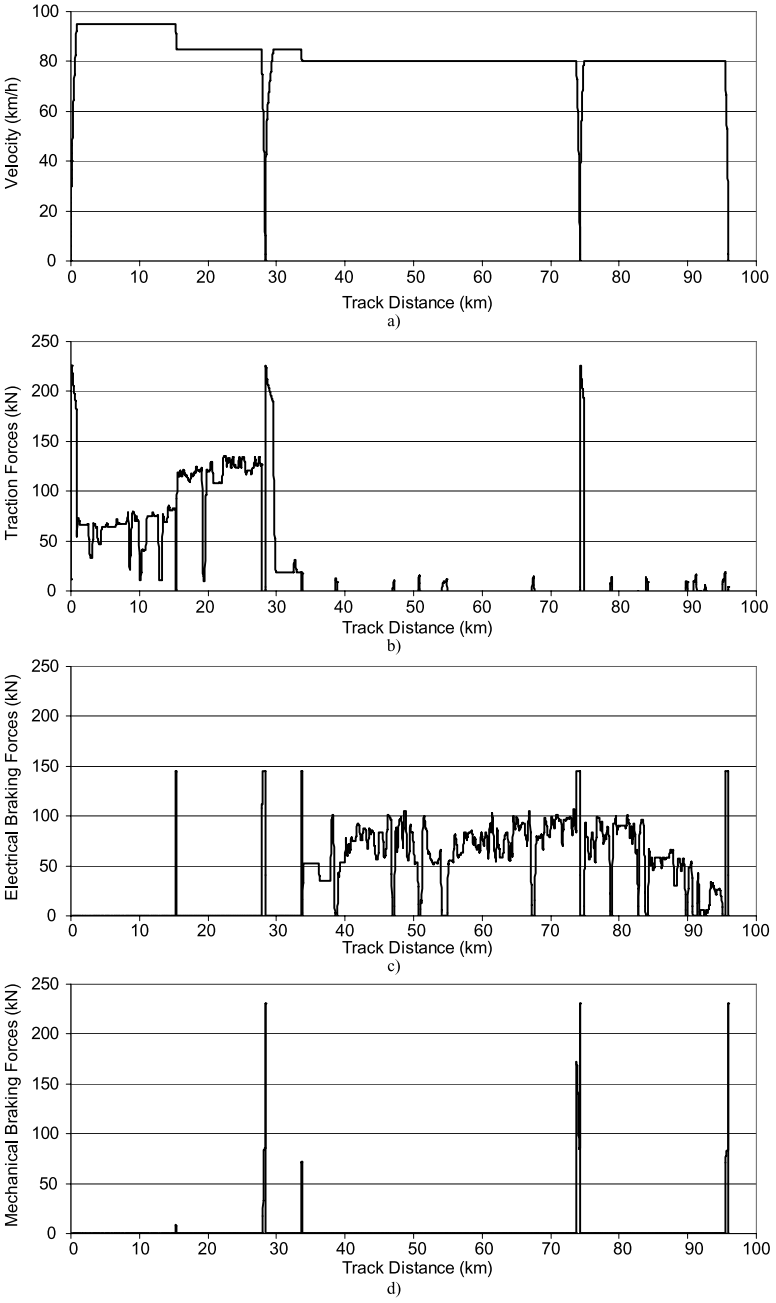


**Fig. 19** Characterization of the traction and braking forces: (**a**) velocity profile; (**b**) traction forces; (**c**) electrical braking forces; (**d**) mechanical braking forces

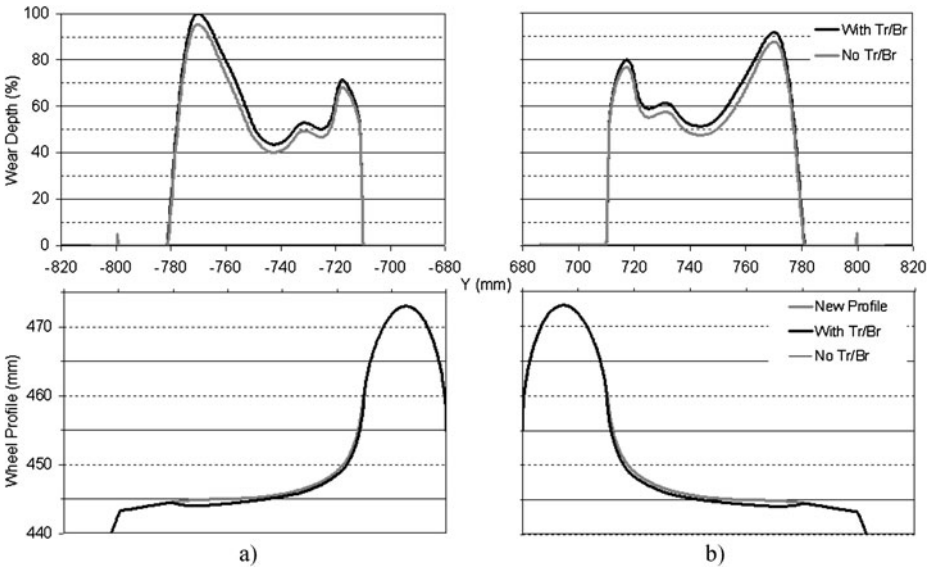


**Fig. 20** Wear results with and without traction/braking forces on: (**a**) *left wheel*; (**b**) *right wheel*

**Table 5** Summary of the influence of traction/braking forces on wear

| Traction/braking | Reprofiling intervals according to wear parameters | | |
|---|---|---|---|
| | Flange height | Flange thickness | Flange slope quota |
| No (Reference) | – | +4.5% | +2.5% |
| Yes (Comparison) | 10.6% | | |

In order to characterize, in a more fundamental way, the influence of the traction/braking forces on the wheel wear growth, the geometry of the worn profiles is analyzed through the wear parameters $Sh$, $Sd$, and $qR$. The comparison of these geometric parameters with the limit values defined by the international standards allows estimating the reprofiling intervals of the wheelsets. The results obtained, using this approach, are summarized in Table 5.

With reference to Fig. 2, the flange height ($Sh$) is the geometrical parameter used to evaluate the wear depth on the wheel tread. On this basis, the variation of the reprofiling intervals based on the analysis of $Sh$ indicates that the traction/braking forces are prejudicial for the tread wear. In fact, when considering these forces, the reprofiling intervals due to problems related to tread wear decrease more than 10%. On the other hand, the analysis of the two geometrical parameters $Sd$ and $qR$ reveals that the traction/braking forces originate slightly higher reprofiling intervals.

The results from Table 5 show that the effect of traction/braking forces on wear regards principally the wheel tread jeopardizing, as expected, the flange height parameter $Sh$ and the equivalent conicity. In general, the increase of $Sh$ by itself enlarges the values of the other wear parameters $Sd$ and $qR$. As a consequence, they became more favorable in terms of reaching their limit values when compared with the case without traction/braking forces. Therefore, in this case $Sh$ is the parameter to consider in the definition of the reprofiling intervals

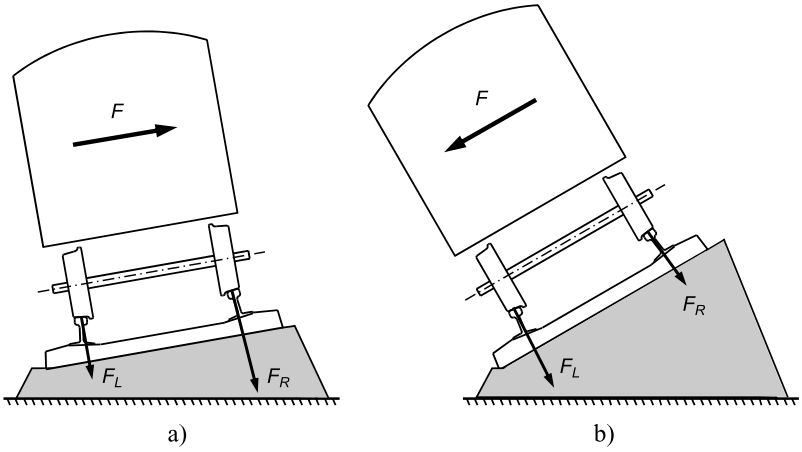


**Fig. 21** Vehicle running with: (**a**) Cant deficiency; (**b**) Cant excess

### 4.4 Influence of vehicle velocity

The objective of this case study is to analyze the wheel wear sensitivity to the service velocity of the railway vehicles. When travelling in curves, the vehicles are subjected to centrifugal accelerations which originate forces that tend to displace them towards outside of the curve. In railway industry, this effect is counteracted by the track cant, i.e., by raising the outer rail with respect to the inner one. This solution reduces the perceived lateral acceleration when negotiating a curve and the respective forces.

The equilibrium cant, for a given curve radius and vehicle speed, corresponds to the value that originates zero track plane acceleration. In general, the track curves are designed to have an equilibrium cant for the nominal velocity conditions of the vehicles that operate on that line. Running in such conditions is advantageous for the passengers since they do not feel the centrifugal accelerations on curves. In addition, the vehicles produce a resultant vertical force through the centreline of the track. Thus, the vertical wheel-rail interaction forces are equal, so that maximum utilization of traction effort and minimum wear on wheels and rails can be realized.

A railway vehicle is running with cant deficiency when its velocity is high enough so that the track cant is not sufficient to assure zero track plane acceleration. In this case, a resultant force $F$ pointing towards the outside of the curve arises, the passengers are pushed in that direction due to the centrifugal force and the vertical contact forces are higher on the outer wheels of the wheelsets, as depicted in Fig. 21a). The opposite happens if, for a given curve radius and vehicle speed, the track cant is higher than necessary to guarantee zero track plane acceleration. In this case, the gravitational force prevails over the centrifugal one and the railway vehicle is said to be running with cant excess, as shown in Fig. 21b).

The study on the influence of the vehicle velocity is performed here by running two wear computations considering the same operation conditions, except the vehicle speed, that has the following values:

- Reference velocity: Varied between 80 and 95 km/h along the Cuneo–Ventimiglia track length, which is in conformity with the service conditions but originates cant deficiency in the majority of the curves;
- Reduced velocity: 45 km/h along the whole track length.

**Table 6** Summary of the influence of vehicle velocity on wear

| Vehicle velocity | Reprofiling interval variation |
|---|---|
| Reference velocity: 80 to 95 km/h<br>Reduced velocity: 45 km/h | +22.7% |

The two comparative wear studies are carried out by performing several outward and return journeys on the Cuneo–Ventimiglia track, which is characterized in Fig. 7, until reaching the total distance of 5000 km. The vehicle model used is Vehicle 2, represented in Fig. 14.

Following the methodology described in the previous case studies, the analysis of the worn profiles of all wheels of Vehicle 2 allows predicting its reprofiling intervals. The results, obtained using this approach, are summarized in Table 6. It is observed that the reduction to half of the vehicle velocity originates an increment of more than 20% in the reprofiling intervals of the vehicle wheelsets.

## 5 Conclusions

In this work, a computational tool that is able to study the dynamic behavior of railway vehicles in realistic operation scenarios and to predict the wheel wear evolution according to those service conditions is presented. The objective is to analyze how the wheel wear progression is affected by some physical parameters related to the vehicle characteristics and to the trainset service conditions. The assessment of the wear sensitivity to these parameters is made according to the international standards. Hence, the wheel wear representation is based on the profile parameters $Sd$, $Sh$, and $qR$. The measurement of these geometrical parameters and its comparison with the limit values allows predicting the reprofiling intervals of the wheelsets.

The comparative study performed here to evaluate the wear sensitivity to the primary suspension stiffness reveals that the vehicle assembled with the softer primary suspension tends to produce less wheel wear on both tread and flange zones. This fact enables it to operate for larger distances before requiring the reprofiling of the wheelsets. These numerical results are in line with the expectations as the track considered here is particularly curved.

The study on how the wheel wear growth is influenced by the rail cant reveals that the reprofiling intervals obtained when running on the track with a rail cant of 1/40 are larger than when travelling on a track with a rail inclination of 1/20. This is a consequence of using a railway vehicle assembled with wheels having a S1002 profile. In fact, this wheel profile has a tread inclination of 1/40 that fits together with the UIC 60 (1/40) rail. In such conditions, the use of a rail cant of 1/40 is advantageous in terms of wheel wear progression. These results are in line with expectations and experience.

The characterization on how the traction/braking forces affect the wheel wear growth reveals that these forces originate more wear on the tread zone of the profiles. The wear computations also show that the negative influence of the traction/braking forces on the tread wear evolution is more relevant than the small benefits obtained for the evolution of the flange wear parameters.

The influence on wheel wear evolution of the vehicle velocity is also studied in this work. The results obtained show that the reduction to half of the vehicle service speed originates an increment of more than 20% in the distance that the railway vehicle is able to run before requiring the reprofiling of its wheelsets.

**Acknowledgements** The work presented here results from the joint research effort between ALSTOM Ferroviaria (IT), University of Sheffield (UK) and Technical University of Lisbon (PT), developed in the scope of the European Project AWARE (Reliable Prediction of the Wear of Railway Wheels). The project is supported by the European Community under the Sixth Framework Programme Marie Curie Actions: Host Fellowships, Transfer of Knowledge (TOK-IAP) with the contract number MTKI-CT-2006–042358.

## References

1. UIC 510-2: Trailing stock: wheels and wheelsets. Conditions concerning the use of wheels of various diameters (2004)
2. AEA Technology plc: VAMPIRE user manual-V 4.32. Derby, UK (2004)
3. British-Rail: Research, introduction to VAMPIRE. AEA Technology plc., London (1997)
4. DeltaRail Group Ltd.: VAMPIRE pro user manual-V 5.02. Derby, UK (2006)
5. Lewis, R., Dwyer-Joyce, R., Olofsson, U., Pombo, J., Ambrósio, J., Pereira, M., Ariaudo, C., Kuka, N.: Mapping railway wheel material wear mechanisms and transitions. J. Rail Rapid Transit **224**, 2041–3017 (2010)
6. Pombo, J., Ambrósio, J., Pereira, M., Lewis, R., Dwyer-Joyce, R., Ariaudo, C., Kuka, N.: Development of a wear prediction tool for steel railway wheels. In: Proceedings of 8th International Conference on Contact Mechanics and Wear of Rail/Wheel Systems (CM2009), Firenze, Italy, September 15–18 (2009)
7. Pombo, J., Ambrósio, J., Pereira, M., Lewis, R., Dwyer-Joyce, R., Ariaudo, C., Kuka, N.: A railway wheel wear prediction tool based on a multibody software, J. Theor. Appl. Mech., **48**(3), (2010)
8. Quost, X., Tassini, N., Lewis, R., Dwyer-Joyce, R., Ariaudo, C., Kuka, N.: Predicting railway wheel wear starting from multibody analysis: a preliminary study. In: Proceedings of 2008 IEEE/ASME Joint Rail Conference (JRC 2008), Wilmington, DE, April 22–24 (2008)
9. Quost, X., Tassini, N., Lewis, R., Dwyer-Joyce, R., Ariaudo, C., Kuka, N.: A numerical model of twin disc test arrangement for evaluating railway wheel wear prediction algorithms. In: Proceedings of the STLE/ASME International Joint Tribology Conference (IJTC 2008), Miami, Florida, October 20–22 (2008)
10. Tassini, N., Quost, X., Lewis, R., Dwyer-Joyce, R., Ariaudo, C., Kuka, N.: A numerical model of twin disc test arrangement for the evaluation of railway wheel wear prediction methods. Wear **268**, 660–667 (2010)
11. Johnson, K.L.: Contact Mechanics. Cambridge University Press, Cambridge (1985)
12. Kalker, J.J.: Survey of wheel-rail rolling contact theory. Veh. Syst. Dyn. **8**(4), 317–358 (1979)
13. Kalker, J.J.: Three-Dimensional Elastic Bodies in Rolling Contact. Kluwer Academic, Dordrecht (1990)
14. Pombo, J., Ambrósio, J.: Application of a wheel-rail contact model to railway dynamics in small radius curved tracks. Multibody Syst. Dyn. **19**(1–2), 91–114 (2008)
15. Pombo, J., Ambrósio, J., Silva, M.: A new wheel-rail contact model for railway dynamics. Veh. Syst. Dyn. **45**(2), 165–189 (2007)
16. Beagley, T.M.: Severe wear of rolling/sliding contact. Wear **36**, 317–335 (1975)
17. Bolton, P.J., Clayton, C.: Rolling—sliding wear damage in rail and tyre steels. Wear **93**, 145–165 (1983)
18. Braghin, F., Lewis, R., Dwyer-Joyce, R., Bruni, S.: A mathematical model to predict railway wheel profile evolution due to wear. Wear **261**, 1253–1264 (2006)
19. Dearden, J.: The wear of steel rails and tyres in railway services. Wear **3**, 43–59 (1960)
20. Enblom, Simulation of railway wheel profile evolution due to wear. In: Proceedings of the SIMPACK User' Meeting (2006)
21. Jendel, T.: Prediction of wheel profile wear—comparisons with field measurements. Wear **253**, 89–99 (2002)
22. Lewis, R., Dwyer-Joyce, R.: Wear mechanisms and transitions in railway wheel steels. J. Eng. Tribol. **218**, 467–478 (2004)
23. Lewis, R., Olofsson, U.: Mapping rail wear regimes and transitions. Wear **257**, 721–729 (2004)
24. Pearce, T., Sherratt, N.: Prediction of wheel profile wear. Wear **144**, 343–351 (1991)
25. Ramalho, A.: A geometrical model to predict the wear evolution of coated surfaces. Wear **264**, 775–780 (2008)
26. Ramalho, A., Miranda, J.: The relationship between wear and dissipated energy in sliding systems. Wear **260**, 361–367 (2006)
27. Haug, E.: Computer Aided Kinematics and Dynamics of Mechanical Systems. Allyn & Bacon, Boston, MA (1989)
28. Nikravesh, P.E.: Computer-Aided Analysis of Mechanical Systems. Englewood Cliffs, Prentice-Hall (1988)

29. Pereira, M., Ambrósio, J.: Computational Dynamics in Multibody Systems. Kluwer Academic, Dordrecht (1995)
30. Roberson, R.E., Schwertassek, R.: Dynamics of Multibody Systems. Springer, Berlin (1988)
31. Schiehlen, W.: Advanced Multibody System Dynamics—Simulation and Software Tools. Kluwer Academic, Dordrecht (1993)
32. Shabana, A.A.: Dynamics of Multibody Systems. 2nd ed. Cambridge University Press, Cambridge (1998)
33. Andersson, E., Berg, M., Stichel, S.: Rail Vehicle Dynamics, Fundamentals and Guidelines. Royal Institute of Technology (KTH), Stockholm (1998)
34. Pombo, J.: A multibody methodology for railway dynamics applications. Ph.D. dissertation, Instituto Superior Técnico, Lisbon, Portugal (2004)
35. UIC 861-3, Profiles Unifiés de Rails à 60 kg. Types UIC 60 et 60 E, 1969
36. Esveld, C.: Modern Railway Track. MRT Productions, Duisburg (1989)
37. UIC 519: Method for determining the equivalent conicity (2004)